

RESEARCH ARTICLE

Comparison of mobility shift affinity capillary electrophoresis and capillary electrophoresis frontal analysis for binding constant determination between human serum albumin and small drugs

Hana Mlčochová^{1,2} | Ratih Ratih^{1,3}  | Lenka Michalcová^{1,2}  |
Hermann Wätzig¹  | Zdeněk Glatz²  | Matthias Stein¹ 

¹Institute of Medicinal and Pharmaceutical Chemistry, TU Braunschweig, Braunschweig, Lower Saxony, Germany

²Department of Biochemistry, Faculty of Science, Masaryk University, Brno, Czech Republic

³Department of Pharmaceutical Chemistry, Faculty of Pharmacy, University of Surabaya, Surabaya, East Java, Indonesia

Correspondence

Matthias Stein, Institute of Medicinal and Pharmaceutical Chemistry, TU Braunschweig, Braunschweig 38106, Lower Saxony, Germany.
Email: matthias.stein@tu-braunschweig.de

Color online: See the article online to view Figures 1 and 2 in color.

Abstract

In this study, two capillary electrophoresis-based ligand binding assays, namely, mobility shift affinity capillary electrophoresis (ms-ACE) and capillary electrophoresis-frontal analysis (CE-FA), were applied to determine binding parameters of human serum albumin toward small drugs under similar experimental conditions. The substances *S*-amlodipine (*S*-AML), lidocaine (LDC), *L*-tryptophan (*L*-TRP), carbamazepine (CBZ), ibuprofen (IBU), and *R*-verapamil (*R*-VPM) were used as the main binding partners. The scope of this comparative study was to estimate and compare both the assays in terms of their primary measure's precision and the reproducibility of the derived binding parameters. The effective mobility could be measured with pooled CV values between 0.55% and 7.6%. The precision of the *r* values was found in the range between 1.5% and 10%. Both assays were not universally applicable. The CE-FA assay could successfully be applied to measure the drugs IBU, CBZ, and LDC, and the interaction toward CBZ, *S*-AML, *L*-TRP, and *R*-VPM could be determined using ms-ACE. The average variabilities of the estimated binding constants were 64% and 67% for CE-FA and ms-ACE, respectively.

KEYWORDS

binding parameters, capillary electrophoresis-frontal analysis, drugs, human serum albumin, mobility shift affinity capillary electrophoresis

Abbreviations: AML, Amlodipine; CE-FA, Capillary electrophoresis-frontal analysis; CBZ, Carbamazepine; D-TRP, D-Tryptophan; HVL, Haarhoff-van der Linde function; IBU, Ibuprofen; LBA, Ligand binding assays; LDC, Lidocaine; *L*-TRP, *L*-Tryptophan; ms, mobility shift; ms-ACE, Mobility shift affinity capillary electrophoresis; NLR, non-linear regression; ODR, non-linear orthogonal distance regression; PRO, Propranolol; SE, Standard errors; STG, Sitagliptin; VPM, Verapamil.

Hana Mlčochová and Matthias Stein are equally contributing authors.

This is an open access article under the terms of the [Creative Commons Attribution-NonCommercial](https://creativecommons.org/licenses/by-nc/4.0/) License, which permits use, distribution and reproduction in any medium, provided the original work is properly cited and is not used for commercial purposes.

© 2022 The Authors. Electrophoresis published by Wiley-VCH GmbH.

1 | INTRODUCTION

During an early stage of drug development, the mechanisms of elimination, the contribution of drug-metabolizing enzymes, the characterization of drug–drug interactions, and the binding to plasma proteins are investigated. These interactions significantly affect pharmacokinetics and pharmacodynamics [1]. The pharmacokinetic describes drug absorption, distribution, metabolism, and excretion. The mechanism of drug action and the relationship between the concentration at its site of action and pharmacologic response can be summarized as pharmacodynamics [2]. Plasma proteins act as a reservoir of the drug and prolong the duration of the drug's effect. As only the free drug fraction can permeate from blood circulation into tissues or organs and provides pharmacological effects, the extent of protein binding is a critical attribute [3]. Human serum albumin (HSA), α 1-acid glycoprotein, and various lipoproteins play a major role in protein–drug interaction. Although HSA binds mostly acidic drugs, α 1-acid glycoprotein is the main carrier for basic and neutral drugs [4].

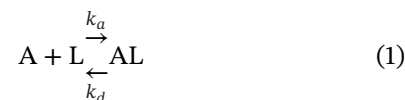
Several ligand binding assays (LBA), such as equilibrium dialysis, ultracentrifugation, parallel artificial membrane permeability assay, high-performance liquid chromatography, surface plasmon resonance, isothermal titration calorimetry, circular dichroism, or various electrophoretic techniques, were developed for studying biomolecular interactions [5, 6]. In contrast to other techniques, CE-based assays provide several benefits such as high separation efficiency, the possibility of automation, low sample consumption, no need for immobilization or labeling of interacting partners, and the opportunity to use different detectors [1, 7]. Due to the high number of versatile CE-based techniques, it can be applied in many situations. A detailed summary of these different approaches was published by Galievsky et al. in 2014 [7].

Mobility shift affinity capillary electrophoresis (ms-ACE) and capillary electrophoresis-frontal analysis (CE-FA) are the most popular CE-based LBAs for studying plasma protein–drug interactions [6]. Unfortunately, the general reliability and the precision of LBAs are often very limited [8, 9]. For this reason, the applicability, as well as the analytical quality of the derived binding parameter, was studied using ms-ACE and CE-FA. Therefore, methods with similar experimental conditions were developed and applied to measure the interaction of HSA with several drugs, including amlodipine (AML), lidocaine (LDC), D-tryptophan (D-TRP), L-tryptophan (L-TRP), carbamazepine (CBZ), ibuprofen (IBU), propranolol (PRO), sitagliptin (STG), and verapamil (VPM). Obtained binding parameters were compared to quantify their reproducibil-

ity and precision as well as to point out the benefits and drawbacks of both assays.

1.1 | Theory of ms-ACE

If an analyte (A) interacts (assuming fast kinetics) with a ligand (L), which is homogeneously distributed in the background electrolyte (BGE), “A” exists in free form and as a complex with the ligand (AL). Assuming the simplest case of a 1:1 stoichiometry, the binding can be expressed as



where k_a and k_d are the association and dissociation rate constants, respectively [7, 10–14].

The strength of the binding reaction is commonly expressed as the value of the association constant (K_A) or the dissociation (K_D) constant, see the following equation:

$$\frac{1}{K_D} = K_A = \frac{k_a}{k_d} = \frac{a(AL)}{a(A) \cdot a(L)} \quad (2)$$

where $a(X)$ denotes the activity of X. In low concentration, the activity equals the concentration and can be replaced [10, 12–16].

In this work's ms-ACE setup, the association constant is obtained by fitting the shift of the drug's effective mobility (μ) and the total HSA concentration (c) to the model equation using nonlinear regression (NLR). Depending on c , μ shifts from the drug's mobility (μ_f) toward the one of the fully saturated complex (μ_c). The standard ms-ACE model is described by the following equation [15]:

$$\mu = \frac{\mu_f + \mu_c \cdot K_A \cdot c}{1 + K_A \cdot c} \quad (3)$$

The above equation is generally valid, but concentration-dependent influences, such as the viscosity, the ionic strength, or the pH of the assay buffer, must be considered. During a measurement series, these experimental conditions must be held as constant as possible, or corrections must be applied [12, 15, 17].

1.2 | Theory of CE-FA

As a matter of fact, the same simple reversible and rapid interaction of A and L as described in Equations (1)

and (2) applies in CE-FA measurements as well. In this assay, a large plug of equilibrated mixture is injected and separated in the electrical field. It leads to the formation of plateau-like peaks, which can be used to estimate the free drug concentration (c_f). The primary measure in CE-FA is the ratio (r) of bound drug concentration (c_b) to total HSA concentration; see the following equation [10, 18–20]:

$$r = \frac{c_b}{c} = \frac{n \cdot K_A \cdot c_f}{1 + K_A \cdot c_f} \quad (4)$$

The c_b can be calculated as the difference between the total drug concentration (c_{tot}) and c_f ; $c_b = c_{\text{tot}} - c_f$. In CE-FA, c_{tot} is defined by the assay and c_f can be estimated from the height (H) of the plateau peaks using a calibration function. The main advantage of CE-FA is the possibility of measuring multiple binding (n : number of binding sites with equal K_A values) and assessing c_f directly. However, if a molecule has multiple binding sites, a model of higher complicity is required [10, 18–20]. The binding parameters K_A and n can be determined by fitting r and c_f to the model equation using NLR or orthogonal distance regression (ODR) [19–23].

2 | MATERIALS AND METHODS

2.1 | Materials

The reagents were obtained by the following suppliers: monopotassium phosphate: Fluka/Riedel-de Haën GmbH (Seelze, Germany); disodium phosphate dihydrate: Fluka; sodium dodecyl sulfate: SERVA Electrophoresis GmbH (Heidelberg, Germany); carbamazepine and verapamil-HCl: TCI Deutschland GmbH (Eschborn, Germany); *S*-amlodipine (*S*-AML): Biozol Diagnostica Vertrieb (Munich, Germany); *R*-verapamil and amlodipine besylate: Sigma-Aldrich Chemie GmbH (Steinheim, Germany); lidocaine-HCl: Fagron GmbH and Co. KG (Glinde, Germany); ibuprofen: Caelo Caesar and Loretz GmbH (Hilden, Germany); sitagliptin phosphate monohydrate: Huikang BoYuan Chemical Tech CO LTD (Beijing, China); methanol and potassium chloride: Thermo Fisher Scientific Inc. (Waltham, USA); acetone, racemic amlodipine besylate, human serum albumin, propranolol-HCl, sodium hydroxide, *L*-tryptophan, and *D*-tryptophan: Sigma-Aldrich Chemie GmbH (Munich, Germany). All aqueous solutions were prepared using deionized water from an Arium Pro UF/VF (Sartorius, Göttingen, Germany). Every reagent was at least of analytical-reagent grade. All capillaries were kindly supplied by Polymicro Technologies (Phoenix, AZ, USA).

2.2 | General

All CE experiments were performed on one of two identical PrinCE-C 760, both equipped with a PDA detector (spectral range: 190–600 nm) and a high voltage power supply (up to 30 kV) from Prince Technologies B.V. (Emmen, the Netherlands). The instruments were operated using the PrinCE DAX 3D software. Both the vial rack and the capillary oven were temperature controlled to $25 \pm 1^\circ\text{C}$. The BGE of every ACE experiment was 0.067-mol/L phosphate buffer pH = 7.40.

2.3 | Mobility shift ACE

2.3.1 | Experimental procedures

Capillary: Bare fused silica, 50- μm id, 375- μm od, total length: 53.5 cm, effective length: 45 cm. Every electropherogram was recorded over the whole spectral range but evaluated using a specific wavelength for every analyte. These wavelengths (nm) are acetone 265, LDC 214, *D*-TRP/*L*-TRP 277, CBZ 285, AML/VPM 240, PRO 290, and STG 210. Sample concentration: 200 $\mu\text{mol/L}$ (*D*-TRP, *L*-TRP, CBZ), 300 $\mu\text{mol/L}$ (LDC, STG, PRO), 400 $\mu\text{mol/L}$ (AML), and 600 $\mu\text{mol/L}$ (VPM) diluted in pure BGE, except the STG and the VPM samples that contained additional 3.6% or 7.2% (v/v) methanol, respectively. The HSA containing BGEs had concentrations of 0, 15, 30, 50, 70, 90, and 110 $\mu\text{mol/L}$. Every new capillary was conditioned using 1-mol/L sodium hydroxide solution (30 min, 1000 mbar), deionized water (10 min, 1000 mbar), and the pure BGE (20 min, 1000 mbar and 20 min, 15 kV). At the beginning of every measurement series the capillary was equilibrated with the HSA containing BGE (20 min, 1000 mbar and 20 min, 15 kV). Injection: hydrodynamically (50 mbar, 6 s). Separation: 15 kV with cathode at the outlet.

Note: A detailed description of the experimental procedures can be found in Section S5.

2.3.2 | Data processing

The absorption versus time data for the electroosmotic flow (EOF) and the analytes wavelength was exported and subsequently analyzed using the program CEVal [17]. With this program, the peaks were fitted to the Haarrhoff–van der Linde (HVL) function and the a_1 parameters were used as absolute mobility. The effective mobility results from the subtraction of the EOFs from the analyte's mobility. The binding parameters were estimated by (weighted) NLR using the ligand concentration as an independent variable, the mean effective mobility as a dependent variable, and

the sample standard deviation (SD) as weights applied to a viscosity corrected ms-ACE model (see Equation S11) [17]. The reported standard errors (SE) result exclusively from the uncertainty of the regression. Additional information about the regression analysis including applied restrictions is listed in Section S2.

2.4 | Frontal analysis (CE-FA)

2.4.1 | Experimental procedures

Capillary: Bare fused silica, 50- μm id, 375- μm od, total length: 43.5 cm, effective length: 35 cm. For all electropherograms, the spectral range from 190 to 600 nm was recorded, but just defined wavelengths were evaluated. These wavelengths (nm) were: LDC 214, L-TRP 220, CBZ 285, IBU 220, AML 240, STG 210, VPM 240, PRO 240. For every measurement series, a ligand (5 mmol/L, except CBZ: 1.2 mmol/L) and an HSA (500 $\mu\text{mol/L}$) stock solution were prepared. Before dilution, IBU was pre-solved in sodium hydroxide (0.1 mol/L) and AML, CBZ, VPM were pre-solved in 15% methanol (v/v). The ligand and stock solutions were used to set up a calibration curve with c ($\mu\text{mol/L}$): 50, 100, 300, 500, 700, and 1000. Every pure ligand sample was measured with two replicates and the estimated plateau heights were fitted to a linear function. The sample solutions were prepared by mixing appropriate volumes of the ligand stock solution, the HSA stock solution, and pure BGE. The final sample solutions contained 50 $\mu\text{mol/L}$ (IBU, AML, STG, VPM) or 75 $\mu\text{mol/L}$ (other substances) HSA and 100, 200, 300, 500, 700, 900, or 1000 $\mu\text{mol/L}$ of the ligands. Every sample was measured with six replicates. New capillaries were conditioned according to the ms-ACE protocol. At the end of every measurement day, the conditioning was refreshed using a reduced version of this method (see Section S5). The sample was injected hydrodynamically (45 mbar, 30 s) followed by a BGE plug of the same length. The separation was performed with 15 kV (cathode at the outlet).

Note: A detailed description of the experimental procedures can be found in Section S5.

2.4.2 | Data processing

The average plateau height and the baseline at this point were evaluated manually using the PrinCE software. The calibration curve was evaluated by ordinary least-squares regression. Using the estimated parameters of the calibration function, c_f of the samples could be estimated from the plateau height. Using this value, r was recalculated.

The mean and SD of c_f and r were calculated for every nominal (total) concentration. As both the independent and the dependent variables are estimated measures and mutually correlated, the binding parameters were estimated using nonlinear ODR [23]. ODR showed higher accuracy in comparison to various types of least squares for data with uncertainties in x for sorption analysis [22]. Therefore, ODR using the means as best estimates and the SD values as weights for both variables were applied. More information about the regression analysis including applied restrictions can be found in Section S2. More information about SE calculation can be found in Section S1 [24].

2.5 | Conductivity measurement

Possible conductivity alterations due to the addition of HSA were measured using a Metrohm Herisau E 518 conductivity meter with a Metrohm Ch-9100 Herisau cell (cell constant = 0.80 cm^{-1}). The instrument was calibrated using five different KCl-solutions with concentrations of 20, 40, 60, 80, and 100 mmol/L. The conductivity of four different BGEs (0, 25, 90, and 120 $\mu\text{mol/L}$) was analyzed.

2.6 | Viscosity measurement

Possible viscosity alterations due to the addition of HSA were measured using a HAAKE RheoStress viscometer (coaxial cylinders: DG41, shear rate: 100–1900 s^{-1} , t : 300 s, steps: 10, step time 30 s, T : 25°C, HAAKE Rheo job manager). The viscosity of five different BGEs (0, 25, 50, 90, and 120 $\mu\text{mol/L}$) was analyzed.

3 | RESULTS AND DISCUSSION

3.1 | Physico-chemical properties of the BGE

3.1.1 | Conductivity

The results of the conductivity measurement are shown in Figure S1A. As the conductivity is linearly dependent on the concentration of charged molecules in solution, the effect of the HSA addition was investigated by linear regression analysis. The linear regression function has the following parameters: intercept: 66.38, SE: 0.62 and slope: -2.58×10^{-3} and SE: 8.06×10^{-3} . According to an ANOVA, the slope does not significantly differ from 0 (significance level: 0.05), which means that the effect of HSA on the conductivity is negligible.

3.1.2 | Viscosity

Figure S1B shows the mean absolute viscosity as a function of the HSA concentration. In theory, protein solutions should show a monotonically exponential viscosity increase with increasing concentration [25–27]. For this reason, the measured viscosity values were fitted to a two-parametric exponential function [$\eta(c) = \exp(\eta_a + \eta_b \cdot c)$]. The parameters η_a and η_b are found to be 12×10^{-3} and 0.27×10^{-3} with SE of 5.4×10^{-3} and 0.073×10^{-3} , respectively.

Note: Additional information about the conductivity and viscosity measurement can be found in Section S3.

3.2 | ms-ACE

In the following section, the complete analysis of the ms-ACE data is presented for the binding pair CBZ/HSA as an example. All other binding pairs were analyzed in the same way, if possible. Complete results are shown in Section S4. Figure 1A shows stacked electropherograms of CBZ in the presence of increasing HSA concentration. Over the ligand range of 0 to 110 $\mu\text{mol/L}$, the measured effective mobility changed from ~ 0 to about $-4.6 \times 10^{-9} \text{ m}^2/\text{V s}$. It could be observed that with increasing ligand concentration, the EOF and all UV signals decreased, and the distortions of both peaks got more pronounced (see Figure 1A). The primary source of the lower sensitivity is an increase of background absorption due to the increasing amount of ligand. The peak distortion toward a triangle shape is a normal behavior of substances in dynamic equilibria [28]. However, as this phenomenon became more pronounced, the computation of the HVL- a_1 parameter needed to be more advanced. At higher ligand levels, a signal dip followed by a peak appeared in the EOF region. The authors assume that the occurrence of this peak is related to differences of the BGE in the EOF zone and the surrounding phases. The overall EOF reduction is very pronounced. On average, the EOF at $c = 0$ is about $45 \times 10^{-9} \text{ m}^2/\text{V s}$ and got reduced to mobilities of about $19 \times 10^{-9} \text{ m}^2/\text{V s}$ at 110 $\mu\text{mol/L}$. This effect is caused by the increase of viscosity in combination with other reasons, such as adsorption of HSA at the capillary wall [29]. The chart in Figure 1B shows the statistical analysis of six replicated measurements performed by three different analysts over the whole ligand range. The absolute pooled SD of the mobility measurement is in the range between 0.024×10^{-9} and $0.108 \times 10^{-9} \text{ m}^2/\text{V s}$. The panel in Figure 1C shows the three independently derived binding curves including their confidence bands and raw data. The binding curve within the ligand range can be described with relatively low measurement uncertainty. From the low observable curvature of

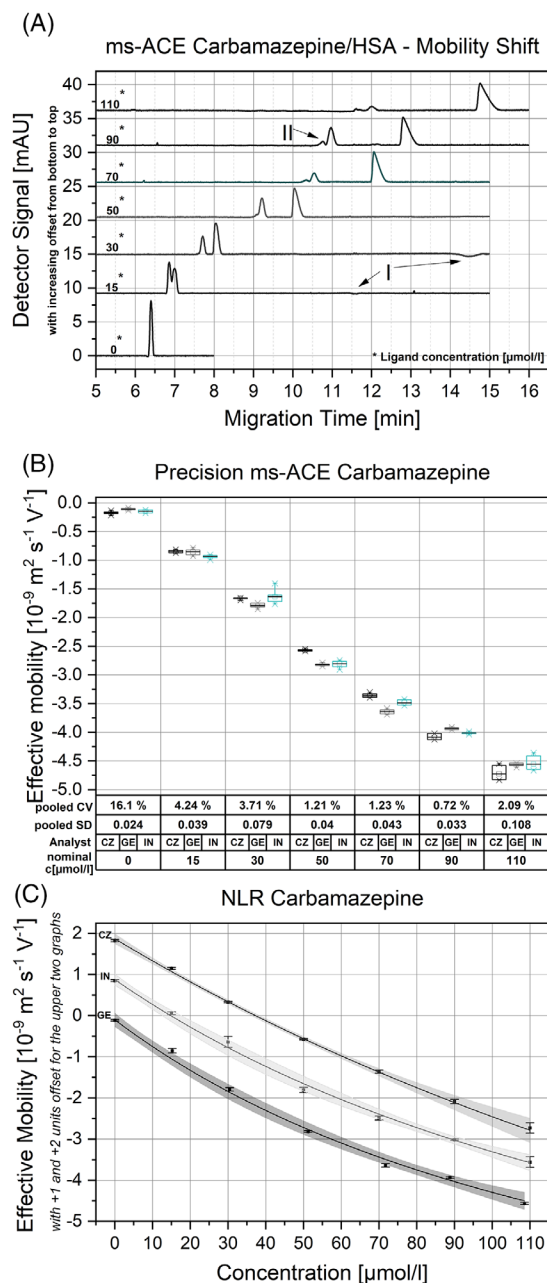


FIGURE 1 Statistical evaluation of mobility shift affinity capillary electrophoresis (ms-ACE) carbamazepine/human serum albumin (HSA): (A) example electropherograms (trace: 285 nm) of every ligand concentration level. The first peak is the electroosmotic flow (EOF) marker acetone and the second one is the analyte carbamazepine: (I) negative dip, (II) alteration of peak shape. (B) Statistical assessment of the mobility measurement for every analyst and ligand concentration. The box shows the 25th–75th percentile, the dotted line marks the mean and the whiskers are indicating the 95% confidence interval. The pooled standard deviation (SD) and coefficient of variation (CV) values of every ligand concentration, the analyst indicator, and the ligand level are listed below the chart. (C) Fitted binding curves of every analyst. The squares indicate the measured mobility including a one SD error bar. The solid line is the best estimate for the binding curve surrounded by a 95% confidence band

the displayed curves (compared to an idealized hyperbola), it can be derived that just a relatively small fraction of it was covered by the ligand range. The low information about the curvature of the binding curve leads coactively to a high measurement uncertainty of the μ_c parameter (see Table S1 rows 7–9) [30]. As the parameters, K_A and μ_c are highly correlated (dependency usually > 0.99), the large uncertainty of μ_c affects the precision of K_A negatively. The measured K_A values cover a range between 2.42×10^3 and 6.03×10^3 L/mol, with relative SEs between 21% and 28% (see Table S1). The μ_f parameter must be treated specially in the case of CBZ. Due to its chemical properties, it is always uncharged, which means it holds no electrophoretic mobility. For this reason, it would be coherent to ignore the $c = 0$ measurement, change the parameter into a constant, and set it to 0. In this study, the ligand-free measurements were treated differently. As shown in Figure 1B the measured uncertainty was about $-0.1 \times 10^{-9} \text{ m}^2/\text{V s}$. As the deviation from 0 is constant in the same direction and has approximately the same magnitude, it was treated as a systematic deviation, which would not affect the determination of the binding parameters. A possible reason for the deviation could be that the mobilities of acetone and CBZ were evaluated at different wavelengths.

3.3 | CE-FA

This section shows the CE-FA measurements of the interaction between IBU and HSA. The same analysis was performed for every other binding pair, if possible. Complete results are shown in Section S4.

As the negative effective mobility of IBU is higher than the one of HSA, the plateau peak appeared at higher migration times compared to the HSA peak. As shown in Figure 2A, H raised with increasing ligand concentration from about 1 to over 10 mAU. Furthermore, it could be observed that the plateaus have rather sharp edges on the right side and diffuse ones on the other side. The reason for this non-sharp front is an ongoing equilibrium reaction with fading ligand concentration in the space between the ligand and analyte zones [13]. Therefore, the H was measured at the rear side of the plateau peaks. Subsequently, the c_f was recalculated from the determined H using beforehand estimated parameters of a linear calibration function (not shown). Figure 2B shows the statistical analysis of the measured r values. For IBU, the r values could be determined with pooled coefficient of variations (CVs) between 0.59% and 1.4%. The binding parameters K_A and n were estimated using nonlinear ODR analysis of the estimated c_f and r data. With this setup, it was possible to describe a large fraction ($\sim 90\%$) of the binding hyperbola

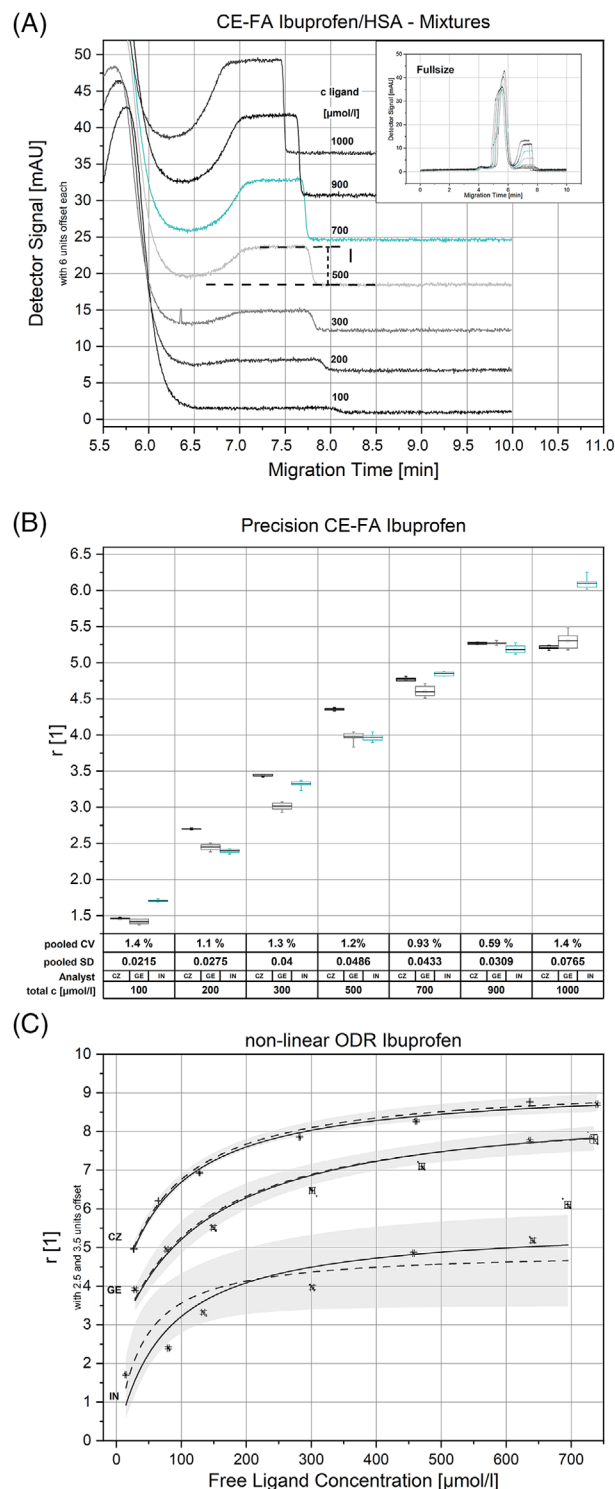


FIGURE 2 Statistical evaluation of capillary electrophoresis-frontal analysis (CE-FA) ibuprofen/human serum albumin (HSA): (A) example electropherogram of every ligand concentration. The total electropherogram is depicted in the upper right corner. The equal sized large peaks belong to HSA, followed by plateau peaks with increasing plateau heights (H). The main picture shows a zoom on the plateau peaks with an offset in y. I: Example for plateau height evaluation. (B) Statistical evaluation of the r -value measurement for every analyst and ligand concentration. The boxes have the size of a 25th–75th percentile, the line inside the box

(see Figure 2C); thus, the range of the estimated parameters is relatively narrow. The range of K_A was estimated to be between 7.05 and 13.5×10^3 L/mol, which translates to K_D values of 74–141 $\mu\text{mol/L}$. The number of maximal binding sites was found in the range between 5.60 and 6.38 (see Table S3). Both of the reported ranges seem to be very large, but in the context of measurement uncertainties in LBA, these results can be regarded as rather precise and reproducible [8, 9].

3.4 | Comparison

The quality of the data was very different among the different analytes. In general, the precision of both the effective mobility and the r values was comparable between the tested drugs. However, the repeatability of the binding parameters was drastically different between the assays and among the drugs. It could be shown that if the respective technique is generally suitable for a specific analyte/ligand pair, then the primary measure can be determined with relatively high precision. For instance, the shifted effective mobilities for CBZ, L-TRP, S-AML, and R-verapamil (R-VPM) were determined with pooled SD values between 0.024×10^{-9} and 0.239×10^{-9} $\text{m}^2/\text{V s}$, which corresponds to pooled CV values between 0.55% and 7.6%. Here, the relative value for $c = 0$ of the CBZ measurement is not regarded, because the mean is close to 0 and thus small SDs can lead to high CVs. The mean of all regarded pooled CV values is 2.2% for both CBZ and L-TRP, and 2.9% for S-AML and R-VPM. In comparison, the r values of the CE-FA measurement for IBU could be determined with pooled SDs between 0.0215 and 0.0765, which is constantly below 1.5% CV. The evaluation of the r values of the CBZ, AML, and LDC assessments showed a lower precision. Their pooled CV values were mainly found in the range between 5% and 10%. The lower precision of AML and CBZ could be related to the organic solvent in the stock solution, which can cause a stacking effect. Another important factor is the percentage of binding. Thus, it is important to choose an appropriate protein concentration for a specific assay. If the binding is too high, the plateau is hard to detect in the lower concentrations. If it is too low, the

absolute bound concentration gets smaller, which affects the precision of the measured differences negatively. All results of the statistical evaluation of the primary measures are summarized in Table 1.

Unfortunately, it was not possible to measure all analytes with both techniques. In fact, only CBZ, L-TRP, S-AML, and R-VPM could be fully analyzed with ms-ACE and IBU, CBZ, S-AML (with limitations) and LDC were completely analyzable with CE-FA. However, qualitative and semiquantitative results such as binding confirmation or relative binding strength could be evaluated for more analytes. Table 2 lists the results for all main drugs that could successfully be measured three times with at least one of the techniques.

The reasons why a molecule is not measurable can be very different. For instance, IBU, as a negatively charged compound, showed negative mobility, which was very similar to the negative dip in the electropherograms (see “I” in Figure 1A). Therefore, it was not possible to detect any IBU peak in the presence of HSA. For LDC, no shift of mobility within a ligand range of 0–50 $\mu\text{mol/L}$ could be measured. It is assumed that the strength of the interaction is too weak to be measured with the described ms-ACE setup. Dissociation constants of over 1000 $\mu\text{mol/L}$ are reported in the literature [19, 31]. The non-suitability of CE-FA for measuring the interaction between HSA and L-TRP is not easily explainable. At certain ligand levels, the free ligand concentration was measured to be higher than the totally applied one. This resulted in negative r values and is obviously not correct. A possible bias, which could lead to those findings, is a disregarded nonlinearity in the calibration curve. This eventually not fully linear relation between c_f and H could be a result of the increasing discrepancy between the physicochemical properties of the sample plug and the surrounding BGE. However, previous studies from Nevídalová et al. [19] proved the general applicability of CE-FA to determine the binding parameters of L-TRP. The main differences between the studies are the applied BGE (borate buffer pH: 8.50), the diameter of the capillary (75 μm), and the instrument (Agilent 3D Capillary Electrophoresis System). The reason why S-VPM was not measurable could be related to a nonlinear behavior of the calibration curve as well. Because of strong deviations from linearity at higher concentrations, the normally applied calibration curve had to be reduced to a maximal concentration of 500 $\mu\text{mol/L}$. The same, but less pronounced, effect could also be present in the lower concentration range.

In summary, it could be shown that the binding properties from 4/6 (IBU, CBZ, S-AML, LDC) of the main pairs were generally measurable with CE-FA and 4/6 (CBZ, S-AML, R-VPM, L-TRP) with ms-ACE. Fortunately, the two non-suitabilities do not overlap and thus all six pairs could

indicates that the mean and the whiskers cover the 95% confidence interval. Both the pooled standard deviation (SD) and coefficient of variation (CV) are listed below every column. (C) Estimated binding curves for every analyst with offset in y . The chart includes the mean values of r and c_f with their respective error bars ($1 \times \text{SD}$) and the best estimates of the curve calculated using nonlinear orthogonal distance regression (ODR) (solid line) and nonlinear regression (NLR) (dotted line) including a 95% confidence band for the NLR fit

TABLE 1 Overview of the precision of the primary measures

	Range pooled SD μ (10^{-9} m ² /V s)	Range pooled CV μ	Remarks	Range pooled SD of r [1]	Range pooled CV of r	Remarks
IBU	NE	NE	–	0.0215–0.0765	0.59%–1.4%	No observable trends
CBZ	0.024–0.108	0.72%–4.24% ($c = 0$: 16.1%)	Near $\mu = 0$ CV \uparrow , no visible trends	0.02–0.0391	2.22%–8.25%	No observable trends
S-AML	0.031–0.218	0.55%–7.6%	Possible trend: var. $\sim c$, not significant	0.046–0.318	6.18%–10.4%	No observable trends
R-VPM	0.063–0.239	0.83%–7.3%	Possible trend: var. $\sim c$, not significant	NE	NE	–
LDC	NE	NE	–	0.032–0.152	9.50%–15.1% ($c = 100$: 27.6%)	Near $R = 0$ CV \uparrow ; possible trend: var. $\sim c$; CV const. not significant
L-TRP	0.0298–0.0991	1.64%–3.10%	possible trend: var. $\sim c$; CV const. not significant	NE	NE	–

Abbreviations: CBZ, carbamazepine; CV, coefficient of variation; IBU, ibuprofen; LDC, lidocaine; L-TRP, L-tryptophan; NE, not evaluable; R-VPM, R-verapamil; S-AML, S-amlodipine; SD, standard deviation.

TABLE 2 Summary of the estimated binding parameter

	Range K_A (10^3 L/mol)			μ_f (10^9 m ² /V s)	μ_c (10^9 m ² /V s)	n	Ref. range K_A (10^3 L/mol)
	ms-ACE	CE-FA					
IBU	NE	7.05–13.5	NE	NE	5.60–6.38	5.2–900 5.5–81 ^b	[19] ^a
CBZ	2.42–6.03	3.15–6.81	–0.129 to –0.100	–22.9 to –11.6	0.871–1.25	5.29–14.1	[36–40]
S-AML	6.77–11.8	0.756	9.68–11.1	–20.2 to –10.7	9.33	90.1–1.59	[41, 42]
R-VPM	2.27–4.85	NE	11.3–12.6	–5.97 to –27.4	NE	67.1–2.67	[43, 44]
LDC	NE	1.47–2.50	NE	NE	1.04–1.97	0.310–1.96	[19] ^a
L-TRP	9.46–14.9	NE	–1.85 to –1.45	–5.51 to –4.60	NE	3.40–44.0	[19] ^a

Abbreviations: CBZ, carbamazepine; CE-FA, capillary electrophoresis-frontal analysis; IBU, ibuprofen; LDC, lidocaine; L-TRP, L-tryptophan; ms-ACE, mobility shift affinity capillary electrophoresis; NE, not evaluable; R-VPM, R-verapamil; S-AML, S-amlodipine.

^aIncl. table in the [supporting material](#).

^bRange of the subset of K_A values where $n > 1.5$.

be assessed using at least one of the techniques. Next to the six main substances, five additional substances were tested. The results of these experiments are given in the [Supporting Information](#) section.

The second-last column of Table 2 lists external reference values from the literature. The shown values mark the minimal and maximal values of the reported constants. Due to the wide variability of the external references, almost all binding constants found (exception: CE-FA, S-AML) do overlap with their respective target range, which means that the binding constants derived by the two proposed methods do not significantly differ from the external literature reference values. However, this is not surprising because the variety of the external reference ranges is very wide. For the two pairs, where both methods could be

applied, the ranges of the CBZ values do match, whereas the ranges of S-AML do not. As the CE-FA result of S-AML neither fits the intern comparison nor the extern references and only one of three evaluations was successful, it is most likely that this result could be incorrect.

The reproducibility of the binding constant determination was estimated from the variability of the determined binding parameters within a series. As the maximal number of replicated measurement series is just 3, the difference in the total range (ΔK_D) is applied as a variability estimator. The ΔK_D of the CE-FA measurements were estimated to be 68, 171, and 280 $\mu\text{mol/L}$ for IBU, CBZ, and LDC, respectively. For ms-ACE, the ΔK_D were found to be 247, 63, 234, and 39 $\mu\text{mol/L}$ for CBZ, S-AML, R-VPM, and L-TRP, respectively. This corresponds to relative ranges

($\Delta K_D/\text{mean}$) of 69%, 74%, and 49% for CE-FA and 94%, 58%, 70%, and 44% for ms-ACE. Thus, it must be deduced that even if the primary response can be measured with relatively low measurement uncertainty, the variability of the derived parameter can be reasonably high. This means that other factors apart from the data quality of the primary measure are playing a crucial role. Regarding ms-ACE, one of the major influences is the data point position and the data point range of the assay [30]. These two factors describe mainly how much of the binding hyperbola can be covered within the ligand range. As the ms-ACE parameter μ_c is highly correlated to the association constant, the K_A value can be estimated with higher certainty, the better μ_c can be assessed. Therefore, it can be assumed that the data quality of the ms-ACE assay can be improved by increasing the ligand range.

Next to the fully quantifiable binding data, it could be shown that both techniques can be used to measure a binding event qualitatively. Especially, the applicability of ms-ACE to measure analyte mixture samples makes it possible to compare primary measures directly. The difference in chemical responses can be used as a semiquantitative result (see, e.g., Figure S11).

3.4.1 | Limitations of the applicability

The main limitations for the applicability of ms-ACE are (i) the non-detectability of IBU in the presence of HSA, and (ii) eventually too weak binding of LDC, D-TRP, STG, PRO, S-VPM, and R-AML. The non-detectability of IBU (or other acidic drugs with high negative μ_f) cannot be solved without changing the method completely. In the case of weak binding, the ligand range must be extended. Unfortunately, 110 $\mu\text{mol/L}$ was the maximum with this setup. In general, a maximal ligand concentration of 10 times the K_D value or higher should be aimed for [3, 32]. However, such high concentrations are unrealistic with this setup. Nevertheless, the usage of coated capillaries could be an option to extend the ligand range. It could be shown that it was possible to successfully measure substances' ligand ranges of $\sim 1 \times K_D$ and even below (calculated as c_{max} divided by the mean of the measured K_D values). In fact, the importance of a large ligand range must be evaluated in relation to the expected shift and the uncertainty of the mobility estimation [30, 33, 34]. As the precision of the estimation was always in the range of $\sim 0.1 \times 10^{-9} \text{ m}^2/\text{V s}$, the relative maximal mobility shift can be estimated as $|\Delta\mu_{c_{\text{max}}}|$ multiplied by 2 to 3 and divided by 0.1. Such approximations for the successfully measured analytes result in values between 40 and 300. These values are generally in accordance with the calculations of Chen et al. and Stein et al. [30, 33, 34]. Furthermore, the μ_f values of the measurable analytes were always higher than $-2 \times 10^{-9} \text{ m}^2/\text{V s}$. Thus, the proposed

method should generally be applicable, if the μ_f value is > -2 and the mobility shift in the absolute maximal HSA concentration is higher than two mobility units. However, the general usability of that exact method is not very broad, but in the case of impure or racemic samples, it can be an alternative for the estimation of protein–drug binding.

In comparison, the ligand range of CE-FA is less restricted as in ms-ACE. However, the potentially necessary addition of organic solvent might lead to a nonlinear behavior of H . Another limitation of CE-FA is related to the percentage of drug bound to the protein [35]. This parameter can be modified either by increasing the protein concentration in the mixed samples or by using more sensitive detection. However, as the protein concentration increases, partial separation of protein and drug may be suppressed and a change in method must follow. In general, neutral and basic drugs have a lower percentage of binding than acidic drugs. Vuignier et al. suggested the use of 40–150 and 150–300 $\mu\text{mol/L}$ for acidic and neutral or basic drugs, respectively. These suggestions are related to CE-FA measurements of bovine serum albumin and small drugs [35]. In this work, a range between 50 and 75 $\mu\text{mol/L}$ was applied. These concentrations could successfully be applied in previous works of Nevídalová et al. [19]. However, this parameter could be a good starting point for optimizations.

4 | CONCLUDING REMARKS

In this study, the usability, as well as the data quality of primary responses and derived parameters, measured with specific ms-ACE and CE-FA methods were compared. For this reason, detailed experimental operating procedures for both methods were developed and used to estimate the interaction between HSA and several different drugs.

Contrary to the initial expectations, not every interaction was measurable with both methods. In fact, only the binding of IBU, CBZ, S-AML, and LDC could be measured with CE-FA and the one of CBZ, S-AML, L-TRP, and R-VPM was measurable with ms-ACE. Thus, neither of the two assays was universally applicable, but all of the six main drugs could be measured with at least one technique. However, the data quality of some determined binding parameters is very limited. Satisfying data quality could only be achieved in the measurement series of IBU, CBZ, and LDC for CE-FA and CBZ, S-AML, R-AML, L-TRP, and R-VPM for ms-ACE. Apart from that, it could be shown that if a method is suitable for a specific substance, then the related primary response can be estimated with relatively high precision. The effective mobility in an ms-ACE measurement could mainly be estimated with CV values below 3%. The r values in CE-FA could be measured with lower, but also acceptable precision. Except for the CVs

of the IBU measurements (<1.5%), most of the found CV values were in the range between 5% and 10%. However, these low to acceptable uncertainties did not necessarily lead to binding parameters of the same quality. The average variabilities of the parameters estimated with CE-FA (64% [69%, 74%, and 49%]) and ms-ACE (67% [94%, 58%, 70% and 44%]) were less precise. Interestingly, the significantly higher precision of the r value measurement in IBU did not lead to a significantly higher reproducibility of the binding constant. Although the binding constant of IBU could be estimated with a variability of 69%, the interaction between HSA and LDC could be determined with a precision of 49%. This leads to the conclusion that other factors, such as the design of the measurement, play a more important role than the precision of the primary measure. For instance, the authors assume that the data quality of the ms-ACE method could remarkably be improved by expanding the applied maximal ligand range.

In summary, the ms-ACE method seems to be generally applicable for drugs with μ_f values >-2 in combination with a relatively high affinity. In contrast, the CE-FA method showed better performance for acidic drugs and comparably lower affinity.

However, the applicability and the data quality of the tested methods are highly dependent on the specific ligand-analyte system. Thus, general statements about these attributes are not possible. But if the conditions are favorable, both methods can be used to measure binding reliably. Accordingly, both methods can be included into the portfolio of LBAs to measure the binding between HSA and small molecules.

ACKNOWLEDGMENTS

The authors thank Polymicro Technologies for providing the capillaries. The authors also thank Sophie Hartung, Finja Krebs, and Holger Zagst for proofreading and helping to edit the manuscript. Parts of this work were supported by grant GA19-08358S from the Czech Science Foundation.

Open Access funding enabled and organized by Projekt DEAL.

CONFLICT OF INTEREST


The authors have declared no conflict of interest.

DATA AVAILABILITY STATEMENT

The data that support the findings of this study are available from the corresponding author upon reasonable request.

ORCID

Ratih Ratih  <https://orcid.org/0000-0002-9308-2281>

Lenka Michalcová  <https://orcid.org/0000-0002-4880-1304>

Hermann Wätzig  <https://orcid.org/0000-0002-7456-0612>

Zdeněk Glatz  <https://orcid.org/0000-0003-3426-6117>

Matthias Stein  <https://orcid.org/0000-0001-9804-2441>

REFERENCES

1. Farcaş E, Pochet L, Crommen J, Servais A-C, Fillet M. Capillary electrophoresis in the context of drug discovery. *J Pharm Biomed Anal.* 2017;144:195–212.
2. Corrie K, Hardman JG. Mechanisms of drug interactions: pharmacodynamics and pharmacokinetics. *Anaesth Intensive Care Med.* 2011;12:156–9.
3. Vuignier K, Veuthey J-L, Carrupt P-A, Schappler J. Global analytical strategy to measure drug-plasma protein interactions: from high-throughput to in-depth analysis. *Drug Discov Today.* 2013;18:1030–4.
4. Nevidalová H, Michalcová L, Glatz Z. In-depth insight into the methods of plasma protein-drug interaction studies: comparison of capillary electrophoresis-frontal analysis, isothermal titration calorimetry, circular dichroism and equilibrium dialysis. *Electrophoresis.* 2018;39:581–9.
5. Nevidalová H, Michalcová L, Glatz Z. Capillary electrophoresis-based approaches for the study of affinity interactions combined with various sensitive and nontraditional detection techniques. *Electrophoresis.* 2019;40:625–42.
6. Olabi M, Stein M, Wätzig H. Affinity capillary electrophoresis for studying interactions in life sciences. *Methods.* 2018;146:76–92.
7. Galievsky VA, Stasheuski AS, Krylov SN. Capillary electrophoresis for quantitative studies of biomolecular interactions. *Anal Chem.* 2015;87:157–71.
8. Kramer C, Kalliokoski T, Gedeck P, Vulpetti A. The experimental uncertainty of heterogeneous public K(i) data. *J Med Chem.* 2012;55:5165–73.
9. Wätzig H, Oltmann-Norden I, Steinicke F, Alhazmi HA, Nachbar M, Abd El-Hady D, et al. Data quality in drug discovery: the role of analytical performance in ligand binding assays. *J Comput Aided Mol Des.* 2015;29:847–65.
10. Vuignier K, Schappler J, Veuthey J-L, Carrupt P-A, Martel S. Drug-protein binding: a critical review of analytical tools. *Anal Bioanal Chem.* 2010;398:53–66.
11. Jiang C, Armstrong DW. Use of CE for the determination of binding constants. *Electrophoresis.* 2010;31:17–27.
12. Beneš M, Zusková I, Svobodová J, Gaš B. Determination of stability constants of complexes of neutral analytes with charged cyclodextrins by affinity capillary electrophoresis. *Electrophoresis.* 2012;33:1032–9.
13. Kanoatov M, Cherney LT, Krylov SN. Extracting kinetics from affinity capillary electrophoresis (ACE) data: a new blade for the old tool. *Anal Chem.* 2014;86:1298–305.
14. Hulme EC, Trevethick MA. Ligand binding assays at equilibrium: validation and interpretation. *Br J Pharmacol.* 2010;161:1219–37.
15. Dubský P, Dvořák M, Ansorge M. Affinity capillary electrophoresis: the theory of electromigration. *Anal Bioanal Chem.* 2016;408:8623–41.
16. Wren SA, Rowe RC, Payne RS. A theoretical approach to chiral capillary electrophoresis with some practical implications. *Electrophoresis.* 1994;15:774–8.

17. Dubský P, Ördögová M, Malý M, Riesová M. CEval: all-in-one software for data processing and statistical evaluations in affinity capillary electrophoresis. *J Chromatogr A*. 2016;1445:158–65.
18. He X, Ding Y, Li D, Lin B. Recent advances in the study of biomolecular interactions by capillary electrophoresis. *Electrophoresis*. 2004;25:697–711.
19. Nevídalová H, Michalcová L, Glatz Z. Applicability of capillary electrophoresis-frontal analysis for displacement studies: effect of several drugs on l-tryptophan and lidocaine binding to human serum albumin. *J Sep Sci*. 2020;43:4225–33.
20. Qian C, Kovalchik KA, MacLennan MS, Huang X, Chen DDY. Mobility-based correction for accurate determination of binding constants by capillary electrophoresis-frontal analysis. *Electrophoresis*. 2017;38:1572–81.
21. Michalcová L, Glatz Z. Comparison of various capillary electrophoretic approaches for the study of drug-protein interaction with emphasis on minimal consumption of protein sample and possibility of automation. *J Sep Sci*. 2015;38:325–31.
22. Poch J, Villaescusa I. Orthogonal distance regression: a good alternative to least squares for modeling sorption data. *J Chem Eng Data*. 2012;57:490–9.
23. Zwolak JW, Boggs PT, Watson LT. Algorithm 869. *ACM Trans Math Softw*. 2007;33:27.
24. Draper NR, Smith H. *Applied regression analysis*. 3rd ed. Hoboken, NJ: Wiley; 1998.
25. Connolly BD, Petry C, Yadav S, Demeule B, Ciaccio N, Moore JM, et al. Weak interactions govern the viscosity of concentrated antibody solutions: high-throughput analysis using the diffusion interaction parameter. *Biophys J*. 2012;103:69–78.
26. Hong T, Iwashita K, Shiraki K. Viscosity control of protein solution by small solutes: a review. *Curr Protein Pept Sci*. 2018;19:746–58.
27. Woldeyes MA, Qi W, Razinkov VI, Furst EM, Roberts CJ. Temperature dependence of protein solution viscosity and protein-protein interactions: insights into the origins of high-viscosity protein solutions. *Mol Pharm*. 2020;17:4473–82.
28. Le Saux T, Varenne A, Gareil P. Peak shape modeling by Haarhoff-Van der Linde function for the determination of correct migration times: a new insight into affinity capillary electrophoresis. *Electrophoresis*. 2005;26:3094–104.
29. Graf M, Galera Garcia R, Wätzig H. Protein adsorption in fused-silica and polyacrylamide-coated capillaries. *Electrophoresis*. 2005;26:2409–17.
30. Stein M, Haselberg R, Mozafari-Torshizi M, Wätzig H. Experimental design and measurement uncertainty in ligand binding studies by affinity capillary electrophoresis. *Electrophoresis*. 2019;40:1041–54.
31. Jia Z, Ramstad T, Zhong M. Determination of protein–drug binding constants by pressure-assisted capillary electrophoresis (PACE)/frontal analysis (FA). *J Pharm Biomed Anal*. 2002;30:405–13.
32. Hein P, Michel MC, Leineweber K, Wieland T, Wettschureck N, Offermanns S, et al., editors. *Practical methods in cardiovascular research*. Berlin/Heidelberg: Springer-Verlag; 2005. p. 723–83.
33. Bowser MT, Chen DDY. Monte Carlo simulation of error propagation in the determination of binding constants from rectangular hyperbolae. 1. Ligand concentration range and binding constant. *J Phys Chem A*. 1998;102:8063–71.
34. Bowser MT, Chen DDY. Monte Carlo simulation of error propagation in the determination of binding constants from rectangular hyperbolae. 2. Effect of the maximum-response range. *J Phys Chem A*. 1999;103:197–202.
35. Vuignier K, Schappler J, Veuthey J-L, Carrupt P-A, Martel S. Improvement of a capillary electrophoresis/frontal analysis (CE/FA) method for determining binding constants: discussion on relevant parameters. *J Pharm Biomed Anal*. 2010;53:1288–97.
36. Kalanur SS, Seetharamappa J, Kalalbandi VKA. Characterization of interaction and the effect of carbamazepine on the structure of human serum albumin. *J Pharm Biomed Anal*. 2010;53:660–6.
37. Kim HS, Wainer IW. Rapid analysis of the interactions between drugs and human serum albumin (HSA) using high-performance affinity chromatography (HPAC). *J Chromatogr B Analyt Technol Biomed Life Sci*. 2008;870:22–26.
38. Kim HS, Hage DS. Chromatographic analysis of carbamazepine binding to human serum albumin. *J Chromatogr B Analyt Technol Biomed Life Sci*. 2005;816:57–66.
39. Maciążek-Jurczyk M, Pawliszyn J. The automatic use of capillary isoelectric focusing with whole column imaging detection for carbamazepine binding to human serum albumin. *J Pharm Biomed Anal*. 2016;127:9–17.
40. Tong Z, Schiel JE, Papastavros E, Ohnmacht CM, Smith QR, Hage DS. Kinetic studies of drug-protein interactions by using peak profiling and high-performance affinity chromatography: examination of multi-site interactions of drugs with human serum albumin columns. *J Chromatogr A*. 2011;1218:2065–71.
41. Liu X, Song Y, Yue Y, Zhang J, Chen X. Study of interaction between drug enantiomers and human serum albumin by flow injection-capillary electrophoresis frontal analysis. *Electrophoresis*. 2008;29:2876–83.
42. Ratih R, Wätzig H, Stein M, El Deeb S. Investigation of the enantioselective interaction between selected drug enantiomers and human serum albumin by mobility shift-affinity capillary electrophoresis. *J Sep Sci*. 2020;43:3960–8.
43. Mallik R, Yoo MJ, Chen S, Hage DS. Studies of verapamil binding to human serum albumin by high-performance affinity chromatography. *J Chromatogr B Analyt Technol Biomed Life Sci*. 2008;876:69–75.
44. Ding Y, Zhu X, Lin B. Study of interaction between drug enantiomers and serum albumin by capillary electrophoresis. *Electrophoresis*. 1999;20:1890–4.

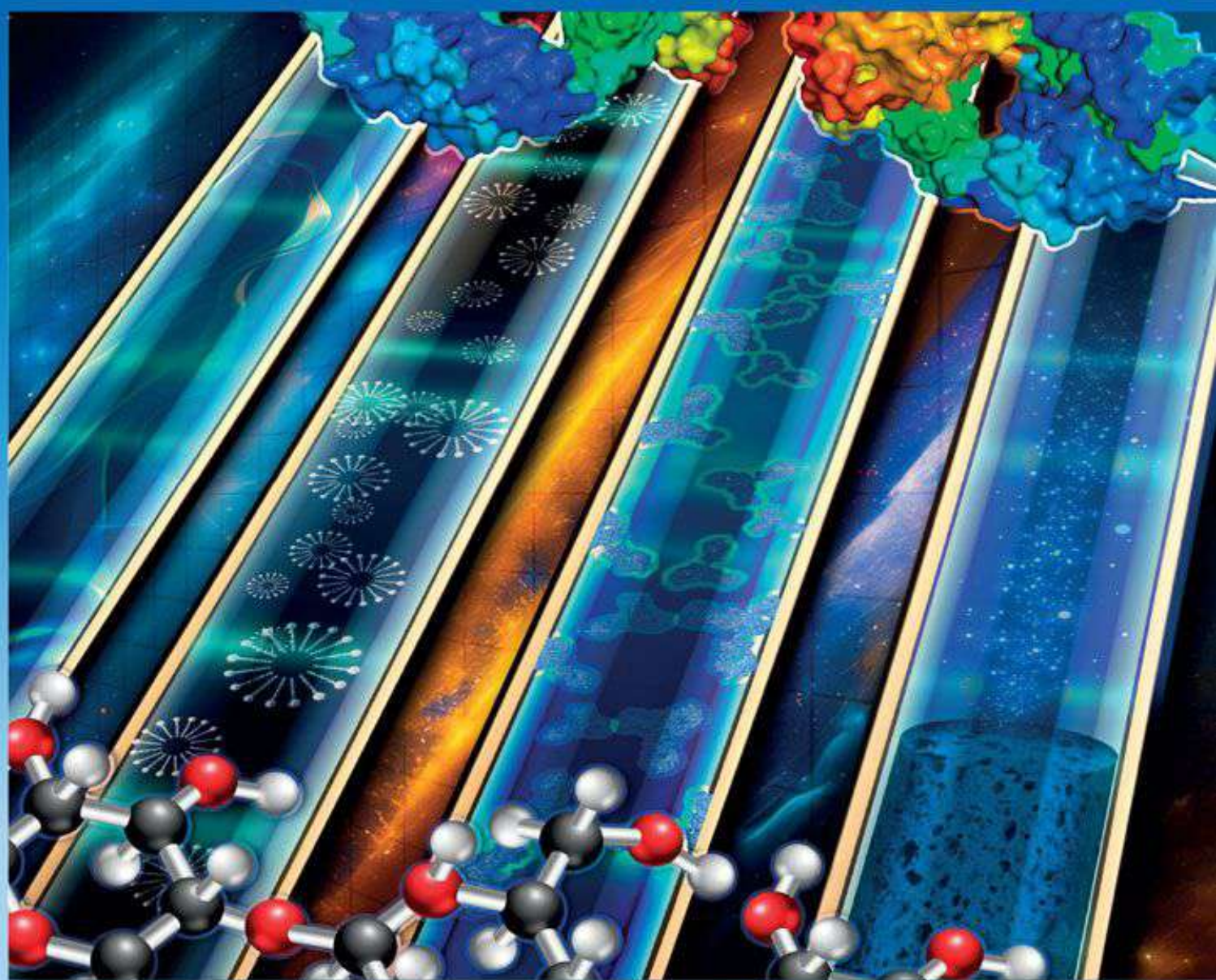
SUPPORTING INFORMATION

Additional supporting information can be found online in the Supporting Information section at the end of this article.

How to cite this article: Mlčochová H, Ratih R, Michalcová L, Wätzig H, Glatz Z, Stein M. Comparison of mobility shift affinity capillary electrophoresis and capillary electrophoresis frontal analysis for binding constant determination between human serum albumin and small drugs. *Electrophoresis*. 2022;1–11.
<https://doi.org/10.1002/elps.202100320>

ELECTROPHORESIS

Electrokinetics  Fluidics  Proteomics **17-18**  **23**



Special Feature

**Mega Review of
Capillary Electrophoresis
Strategies**

www.electrophoresis-journal.com

WILEY  **VCH**

ELECTROPHORESIS

Editors-in-Chief

Blanca H. Lapizco-Encinas (Rochester)
Hermann Wätzig (Braunschweig)

Senior Deputy Editors

František Foret (Brno) Carlos Garcia (Clemson)

Deputy Editors

Emanuel Carrilho (Sao Paulo) Mark Hayes (Tempe) Cari Sänger - van de Griend (Baarn)
Yi Chen (Beijing) Peter Jungblut (Berlin) Athina Vidaki (Rotterdam)
Alejandro Cifuentes (Madrid) Christian Klampfl (Linz) Xiangchun (Schwan) Xuan (Clemson)
Prashanta Dutta (Pullman) Jörg P. Kutter (Copenhagen)
Bohuslav Gaš (Prague) Bruce McCord (Miami)

Founding Editor

Bertold J. Radola (München)

Honorary Editor-in-Chief

Ziad El Rassi (Stillwater)

Honorary Editors

Petr Boček (Brno) Terry M. Phillips (Bethesda)
Bingcheng Lin (Dalian) Andreas M. Rizzi (Wien)
Takashi Manabe (Matsuyama) Nancy C. Stellwagen (Iowa City)

Editorial Board

D. W. Armstrong (Arlington) D. Josic (Providence) Y. Ren (Harbin)
D. Belder (Leipzig) G. Y. Jung (Gyeongbuk) J. Ren (Shanghai)
M. Breadmore (Hobart) B. L. Karger (Boston) M.-L. Riekkola (Helsinki)
B. Buszewski (Torun) Y. Kang (Chongqing) P. G. Righetti (Milano)
B. Chankvetadze (Tbilisi) V. Kašička (Prague) A. Ros (Tempe)
D. D. Y. Chen (Vancouver) F. Kilár (Pécs) G. Rozing (Waldbronn)
S.-H. Chen (Tainan) T. Kitamori (Tokyo) R. R. Rustandi (Kenilworth)
D. S. Chung (Seoul) L. Křivánková (Brno) G. Scriba (Jena)
H. Cottet (Montpellier) M. Lämmerhofer (Vienna) S. A. Shamsi (Atlanta)
R. Davalos (Blacksburg) J. Landers (Charlottesville) K. Shimura (Fukushima)
A. Escarpa (Madrid) K. Lee (Newark) G. W. Slater (Ontario)
C. Fanali (Roma) S. F. Y. Li (Singapore) F. Svec (Berkeley)
J. P. Foley (Philadelphia) Z. Liu (Nanjing) W. Thormann (Bern)
C. Gerner (Vienna) G. Lubec (Vienna) A. Timerbaev (Moscow)
E. Gianazza (Milano) M. Macka (Hobart) O. Trapp (München)
H. H. Girault (Lausanne) Y. Mechref (Lubbock) A. Van Schepdael (Leuven)
C. M. Grgicak (New Jersey) C. Neusüß (Aalen) S. Wiedmer (Helsinki)
A. Guttman (Debrecen) J. Østergaard (Copenhagen) N. Xiang (Nanjing)
N. A. Guzman (Princeton) P. Peluso (Sassari) X.-X. Zhang (Beijing)
P. R. Haddad (Hobart) V. H. Perez-Gonzalez (Monterrey) C. Yan (Shanghai)
P. Hauser (Basel) M. Pumera (Tsukuba) X.-P. Yan (Tianjin)
A. Herr (Berkeley) J. Qin (Dalian) C. Yang (Singapore)
M. Herrero (Madrid) F. Qu (Beijing) G. Yossifon (Haifa)
H. Hirano (Yokohama) R. Ramautar (Leiden) C. Zhao (Xi'an)
T. Hirokawa (Higashi-Hiroshima) A. S. Rathore (New Delhi)

Managing Editor

Danielle Flemming
E-mail: elpho@wiley.com

ELECTROPHORESIS

Electrokinetics
Fluidics
Proteomics**Volume 43, Issue 16-17**

Pages: 1663-1799

September 2022

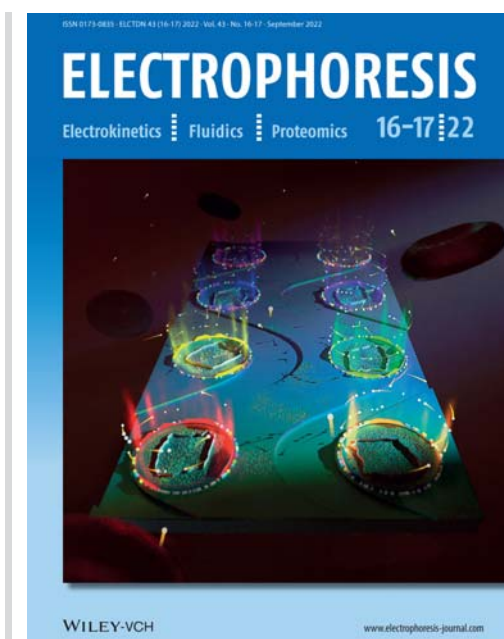
[< Previous Issue](#) | [Next Issue >](#)[☰ GO TO SECTION](#)[🗉 Export Citation\(s\)](#)

COVER PICTURE

[🔒 Free Access](#)**Front Cover: cyc-DEP: Cyclic immunofluorescence profiling of particles collected using dielectrophoresis**

Kyle T. Gustafson, Zeynep Sayar, Hillary Le, Steven L. Gustafson, Austin Gower, Augusta Modestino, Stuart Ibsen, Michael J. Heller, Sadik Esener, Sebnem E. Eksi

First Published: September 2022



DOI: 10.1002/elps.202200001

The cover picture shows the collection of endogenous nanoparticles from blood using a dielectrophoretic chip that consists of a planar microelectrode array. Downstream immunolabeling reveals the diverse proteomic content of captured particles, represented by a spectrum of colors fluorescing at collection regions on the chip. Our group developed a technique called “cyc-DEP” to improve the multiplicity of on-chip proteomic analysis in what we believe is the first application of cyclic immunofluorescence for profiling liquid biopsies. Techniques like cyc-DEP showcase the potential utility of low-volume, minimally-invasive, lab-on-a-chip platforms for patient stratification in routine screening and early disease detection.

[Abstract](#) | [PDF](#) | [Request permissions](#)

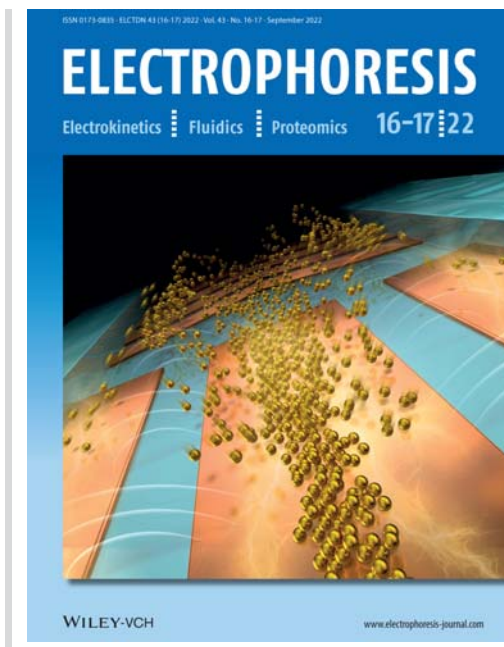
BACK COVER

[Free Access](#)

Back Cover: Efficient nanoparticle focusing utilizing cascade AC electroosmotic flow

Ahmed Abdelghany, Keiichi Yamasaki, Yoshiyasu Ichikawa, Masahiro Motosuke

First Published: September 2022



DOI: [10.1002/elps.202200054](https://doi.org/10.1002/elps.202200054)

The cover picture shows continuous focusing of nanoscale samples using a cascade AC electroosmosis (cACEO) flow. ACEO flow is produced by applying AC signal to the coplanar integrated electrode. The cascade electrode, combining chevron and double-gap geometry, was developed to perform efficient 3D nanoparticle focusing. Chevron electrode was used to generate inward flow from the sidewall to the center area to accumulate particles from the scattering area; then, the DG electrode provides the necessary ACEO to concentrate nanoparticles. The study shows that the cACEO concentrator holds significant potential to concentrate nanoscale samples, such as particles, rare samples, and biomaterials.

[Abstract](#) | [PDF](#) | [Request permissions](#)

EDITORIAL BOARD

[Free Access](#)

Editorial Board: Electrophoresis 16–17'22

Pages: 1663 | First Published: September 2022

[PDF](#) | [Request permissions](#)

CONTENTS

Contents: Electrophoresis 16–17'22

Pages: 1664-1665 | First Published: September 2022

[PDF](#) | [Request permissions](#)

SPOTLIGHT ON REVIEWS 2022

Microfluidic systems for the analysis of blood-derived molecular biomarkers

Oriana G. Chavez-Pineda, Roberto Rodriguez-Moncayo, Diana F. Cedillo-Alcantar, Pablo E. Guevara-Pantoja, Josue U. Amador-Hernandez, Jose L. Garcia-Cordero

Pages: 1667-1700 | First Published: 29 June 2022

[Abstract](#) | [Full text](#) | [PDF](#) | [References](#) | [Request permissions](#)

GENERAL, CE & CEC

Dual-detection approach for a charge variant analysis of monoclonal antibody combination products using imaged capillary isoelectric focusing

Jason Candreva, Abbie L. Esterman, Derek Ge, Pritesh Patel, Shannon C. Flagg, Tapan K. Das, Xue Li

Pages: 1701-1709 | First Published: 30 May 2022

[Abstract](#) | [Full text](#) | [PDF](#) | [References](#) | [Request permissions](#)

Preparation of a zeolite imidazole skeleton–silica hybrid monolithic column for amino acid analysis via capillary electrochromatography

Shili Qin, Hongshou Cui, Hongtao Chu, Lidi Gao, Xue Li, Yimin Tang, Xingyu You, Qing Dong

Pages: 1710-1723 | First Published: 26 May 2022

[Abstract](#) | [Full text](#) | [PDF](#) | [References](#) | [Request permissions](#)

 [Open Access](#)

Comparison of mobility shift affinity capillary electrophoresis and capillary electrophoresis frontal analysis for binding constant determination between human serum albumin and small drugs

Hana Mlčochová, Ratih Ratih, Lenka Michalcová, Hermann Wätzig, Zdeněk Glatz, Matthias Stein

Pages: 1724-1734 | First Published: 15 June 2022

[Abstract](#) | [Full text](#) | [PDF](#) | [References](#) | [Request permissions](#)

The two-phase amphiphilic preconcentration based on surfactants to enrich phenolic compounds from diluted plant extracts and rat urine by micellar electrokinetic chromatography

Ya-Ling Yu, Min-Zhen Shi, Si-Chen Zhu, Jun Cao

Pages: 1735-1745 | First Published: 25 June 2022

[Abstract](#) | [Full text](#) | [PDF](#) | [References](#) | [Request permissions](#)

MINIATURIZATION

[Open Access](#)

Rapid, inexpensive fabrication of electrophoretic microdevices for fluorescence detection

Daniel A. Nelson, Brandon L. Thompson, An-Chi Scott, Renna Nouwairi, Christopher Birch, Jacquelyn A. DuVall, Delphine Le Roux, Jingyi Li, Brian E. Root, James P. Landers

Pages: 1746-1754 | First Published: 03 June 2022

[Abstract](#) | [Full text](#) | [PDF](#) | [References](#) | [Request permissions](#)

[Open Access](#)

Efficient nanoparticle focusing utilizing cascade AC electroosmotic flow

Ahmed Abdelghany, Keiichi Yamasaki, Yoshiyasu Ichikawa, Masahiro Motosuke

Pages: 1755-1764 | First Published: 23 June 2022

[Abstract](#) | [Full text](#) | [PDF](#) | [References](#) | [Request permissions](#)

NUCLEIC ACIDS

Forensic efficacy evaluation and genetic structure exploration of the Yunnan Miao group by a multiplex InDel panel

Xuebing Chen, Shengjie Nie, Liping Hu, Yating Fang, Wei Cui, Hui Xu, Congying Zhao, Bo-Feng Zhu

Pages: 1765-1773 | First Published: 16 June 2022

[Abstract](#) | [Full text](#) | [PDF](#) | [References](#) | [Request permissions](#)

An efficient ancestry informative SNPs panel for further discriminating East Asian populations

Yueyan Cao, Qiang Zhu, Yuguo Huang, Xi Li, Yifan Wei, Haoyu Wang, Ji Zhang

Pages: 1774-1783 | First Published: 24 June 2022

[Abstract](#) | [Full text](#) | [PDF](#) | [References](#) | [Request permissions](#)

PROTEINS, PROTEOMICS AND 2D

[Open Access](#)

cyc-DEP: Cyclic immunofluorescence profiling of particles collected using dielectrophoresis

Kyle T. Gustafson, Zeynep Sayar, Hillary Le, Steven L. Gustafson, Austin Gower, Augusta Modestino, Stuart Ibsen, Michael J. Heller, Sadik Esener, Sebnem E. Eksi

Pages: 1784-1798 | First Published: 26 June 2022

[Abstract](#) | [Full text](#) | [PDF](#) | [References](#) | [Request permissions](#)

CALL FOR PAPERS

Call for Papers

Pages: 1799 | First Published: September 2022

[PDF](#) | [Request permissions](#)

Sign up for email alerts

Enter your email to receive alerts when new articles and issues are published.

Email address*

Continue

More from this journal

[Best Student Paper](#)
[Call for Papers](#)
[Electrophoresis Societies](#)
[Membership Information](#)
[Virtual Issues](#)
[Video Abstracts](#)
[Lectures](#)

Electrophoresis

COUNTRY

Germany



Universities and research
institutions in Germany



Media Ranking in Germany

SUBJECT AREA AND CATEGORY

Biochemistry, Genetics and
Molecular Biology
Biochemistry
Clinical Biochemistry

Chemistry
Analytical Chemistry

PUBLISHER

Wiley-VCH Verlag

H-INDEX



164

PUBLICATION TYPE	ISSN	COVERAGE	INFORMATION
Journals	01730835, 15222683	1980-2022	Homepage How to publish in this journal bhlbme@rit.edu

SCOPE

ELECTROPHORESIS is an international journal that publishes original manuscripts on all aspects of electrophoresis, and liquid phase separations (e.g., HPLC, micro- and nano-LC, UHPLC, micro- and nano-fluidics, liquid-phase micro-extractions, etc.). Topics include new or improved analytical and preparative methods, sample preparation, development of theory, and innovative applications of electrophoretic and liquid phase separations methods in the study of nucleic acids, proteins, carbohydrates natural products, pharmaceuticals, food analysis, environmental species and other compounds of importance to the life sciences. Papers in the areas of microfluidics and proteomics, which are not limited to electrophoresis-based methods, will also be accepted for publication. Contributions focused on hyphenated and omics techniques are also of interest. Proteomics is within the scope, if related to its fundamentals and new technical approaches. Proteomics applications are only considered in particular cases. Papers describing the application of standard electrophoretic methods will not be considered. Papers on nanoanalysis intended for publication in ELECTROPHORESIS should focus on one or more of the following topics: • Nanoscale electrokinetics and phenomena related to electric double layer and/or confinement in nano-sized geometry • Single cell and subcellular analysis • Nanosensors and ultrasensitive detection aspects (e.g., involving quantum dots, "nanoelectrodes" or nanospray MS) • Nanoscale/nanopore DNA sequencing (next generation sequencing) • Micro- and nanoscale sample preparation • Nanoparticles and cells analyses by dielectrophoresis • Separation-based analysis using nanoparticles, nanotubes and nanowires.

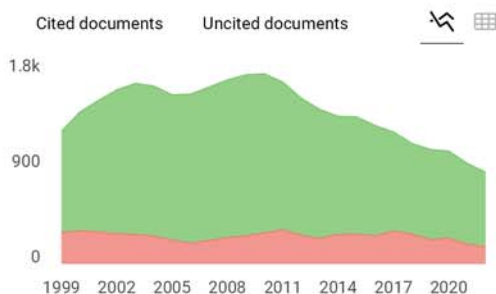
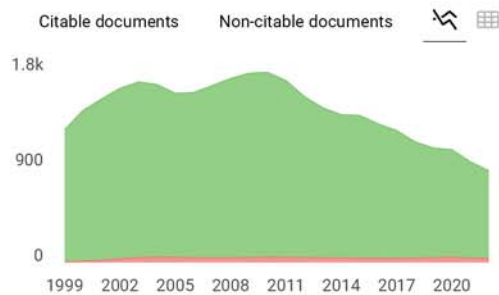
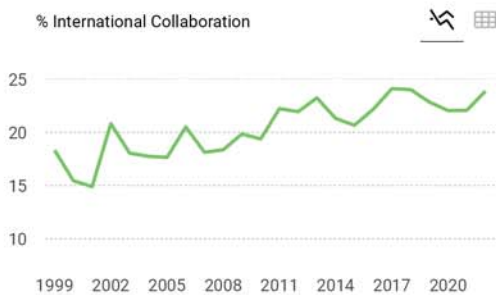
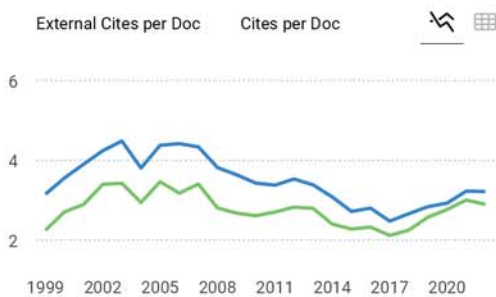
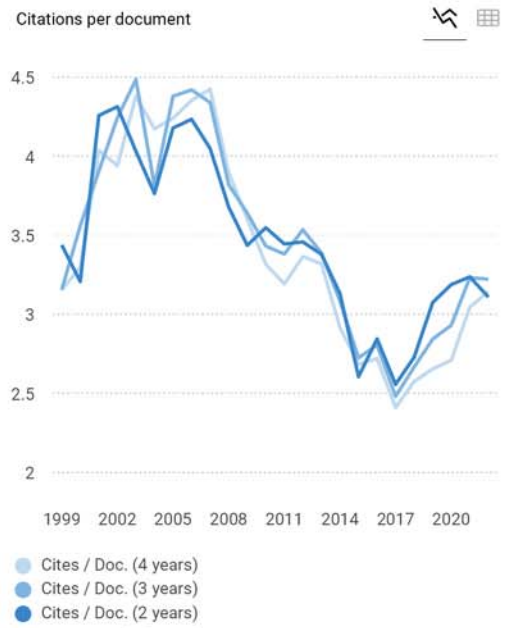
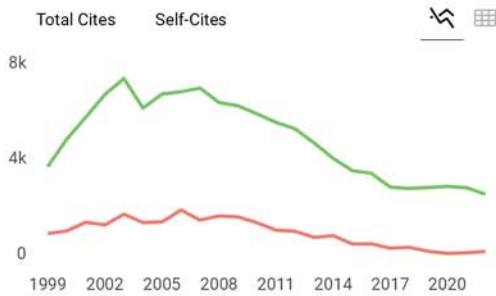
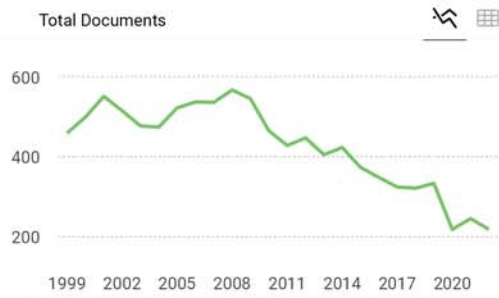
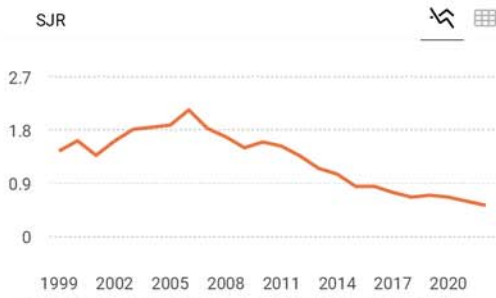
 Join the conversation about this journal

 Quartiles


FIND SIMILAR JOURNALS

<p>1 TrAC - Trends in Analytical Chemistry NLD</p> <p>48% similarity</p>	<p>2 Analytica Chimica Acta NLD</p> <p>46% similarity</p>	<p>3 Analytical and Bioanalytical Chemistry DEU</p> <p>44% similarity</p>	<p>4 Mass Spectrometry Let KOR</p> <p>44% similarity</p>
---	--	--	---





Electrophoresis

Q2 Analytical Chemistry
best quartile

SJR 2022
0.53

powered by scimagojr.com

← Show this widget in your own website

Just copy the code below and paste within your html code:

```
<a href="https://www.scimagojr.com" style="border: 1px solid #ccc; padding: 2px 5px; display: inline-block;">https://www.scimagojr.com
```

SCImago Graphica

Explore, visually communicate and make sense of data with our [new data visualization tool](#).



Metrics based on Scopus® data as of April 2023

Leave a comment

Name

Email

(will not be published)

Submit

The users of Scimago Journal & Country Rank have the possibility to dialogue through comments linked to a specific journal. The purpose is to have a forum in which general doubts about the processes of publication in the journal, experiences and other issues derived from the publication of papers are resolved. For topics on particular articles, maintain the dialogue through the usual channels with your editor.

Developed by:



Powered by:



Follow us on @ScimagoJR

Scimago Lab, Copyright 2007-2022. Data Source: Scopus®

EST MODUS IN REBUS
Horatio (Saturne 1.1.106)





Source details

Electrophoresis

Scopus coverage years: from 1980 to Present

Publisher: Wiley-Blackwell

ISSN: 0173-0835 E-ISSN: 1522-2683

Subject area: [Biochemistry, Genetics and Molecular Biology: Clinical Biochemistry](#) [Biochemistry, Genetics and Molecular Biology: Biochemistry](#)

Source type: Journal

[View all documents >](#)

[Set document alert](#)

[Save to source list](#) [Source Homepage](#)

CiteScore 2022

6.6



SJR 2022

0.527



SNIP 2022

0.842



[CiteScore](#) [CiteScore rank & trend](#) [Scopus content coverage](#)

CiteScore 2022 ▾

$$6.6 = \frac{6,273 \text{ Citations } 2019 - 2022}{957 \text{ Documents } 2019 - 2022}$$

Calculated on 05 May, 2023

CiteScoreTracker 2023 ⓘ

$$5.6 = \frac{4,169 \text{ Citations to date}}{741 \text{ Documents to date}}$$

Last updated on 05 September, 2023 • Updated monthly

CiteScore rank 2022 ⓘ

Category	Rank	Percentile
Biochemistry, Genetics and Molecular Biology	#42/113	63rd
↳ Clinical Biochemistry		
Biochemistry, Genetics and Molecular Biology	#160/428	62nd
↳ Biochemistry		

[View CiteScore methodology >](#) [CiteScore FAQ >](#) [Add CiteScore to your site ↗](#)

About Scopus

[What is Scopus](#)

[Content coverage](#)

[Scopus blog](#)

[Scopus API](#)

[Privacy matters](#)

Language

[日本語版を表示する](#)

[查看简体中文版本](#)

[查看繁體中文版本](#)

[Просмотр версии на русском языке](#)

Customer Service

[Help](#)

[Tutorials](#)

[Contact us](#)

ELSEVIER

[Terms and conditions](#) ↗ [Privacy policy](#) ↗

Copyright © Elsevier B.V. ↗ . All rights reserved. Scopus® is a registered trademark of Elsevier B.V.

We use cookies to help provide and enhance our service and tailor content. By continuing, you agree to the use of cookies ↗.

